

# Multi-omics integration identifies *MT2A* as a biomarker and a candidate host target linking zinc dysregulation to COVID-19 mortality

Zhonghua Li<sup>1,2#</sup>, Siqi Hua<sup>1#</sup>, Shuangshuang Song<sup>1</sup>, Yixiang Luo<sup>3</sup>, Wei Qian<sup>2</sup>, Lina Liu<sup>4\*</sup>, Jiahuang Li<sup>1\*</sup> and Bo Zhu<sup>1\*</sup>

<sup>1</sup> School of Biopharmacy, China Pharmaceutical University, Nanjing 211198, China

<sup>2</sup> Department of Biostatistics, School of Science, China Pharmaceutical University, Nanjing 211198, China

<sup>3</sup> School of Basic Medicine and Clinical Pharmacy, China Pharmaceutical University, Nanjing 211198, China

<sup>4</sup> Peter Gorer Department of Immunobiology, School of Immunology and Microbial Sciences, King's College London, London, SE1 9RT, UK

# Authors contributed equally: Zhonghua Li, Siqi Hua

\* Correspondence: [lina.liu@kcl.ac.uk](mailto:lina.liu@kcl.ac.uk) (Liu L); [lijiah@cpu.edu.cn](mailto:lijiah@cpu.edu.cn) (Li J); [zhubo@cpu.edu.cn](mailto:zhubo@cpu.edu.cn) (Zhu B)

## Abstract

Identifying host programs that connect micronutrient biology to COVID-19 immunopathology may enable more precise host-directed strategies. Zinc deficiency is linked to worse outcomes, yet the intracellular mediators that couple metal/redox stress to disease severity remain unclear. In this study, a PRISMA-guided meta-analysis of zinc supplementation was performed in hospitalized COVID-19 (seven studies; 1,972 participants), and observed reduced mortality (OR 0.48, 95% CI 0.36–0.64). Statistical heterogeneity was low, although regimens varied substantially in formulation, elemental dose, route, and duration. The study then integrated single-cell and bulk transcriptomes across blood and respiratory compartments, to map zinc-homeostasis pattern across disease states. In a large single-cell atlas (GSE158055; 1,462,702 cells from 196 individuals) spanning PBMC, bronchoalveolar lavage fluid, sputum, in bulk RNA-seq from postmortem lung tissue (GSE183533), and longitudinal peripheral blood (GSE198449), *MT2A* showed the most reproducible association with disease severity among metallothioneins, and was enriched in myeloid lineages. Its associations were compartment- and state-dependent, and SARS-CoV-2-relevant entry/processing and innate-sensing are involved, including *TMPRSS2*, *CTSB/CTSL*, and RNA-sensing pathways. In a longitudinal subset with complete timepoints ( $n = 9$ ; days 0, 1, 8, and 12), *MT2A* peaked early after infection and declined thereafter, consistent with an inducible acute-phase response. Together, these results prioritize *MT2A* as a cross-compartment marker of metal/redox immune stress and a testable host node for biomarker-guided stratification and intervention timing, pending perturbation-based causal validation.

**Citation:** Li Z, Hua S, Song S, Luo Y, Qian W, et al. 2026. Multi-omics integration identifies *MT2A* as a biomarker and a candidate host target linking zinc dysregulation to COVID-19 mortality. *Targetome* 2(1): e006 <https://doi.org/10.48130/targetome-0026-0006>

## Introduction

Drug discovery for emerging viral infections increasingly prioritizes host-directed strategies that remain effective despite viral mutation<sup>[1]</sup>. The appeal is clear, but the bar is high. A useful host target needs to sit at the interface of viral entry and the immune dysregulation that drives severe disease, and it must remain actionable for pharmacologic modulation<sup>[2]</sup>.

Zinc is a ubiquitous micronutrient fundamental to antiviral immunity and redox control<sup>[3,4]</sup>. Clinically, low serum zinc has been repeatedly associated with worse outcomes in COVID-19<sup>[5,6]</sup>. While serum zinc measurements do capture systemic status, they tell us relatively little about what happens inside the cell, specifically, how zinc availability gets converted into actual immune phenotypes<sup>[7]</sup>. For this reason, this study's focus is on an intracellular 'targetome': The collection of zinc-buffering proteins and redox-responsive systems that appear to kick in when inflammatory stress is triggered.

Among these proteins, metallothioneins (MTs) stand out. These are cysteine-rich molecules that grab onto zinc with remarkable affinity, and they function like dynamic zinc reservoirs inside cells while also regulating redox balance through their thiol groups<sup>[3]</sup>. *MT2A* in particular has been characterized as a kind of integration point, it seems to connect zinc metabolism with the cellular response to oxidative stress<sup>[8]</sup>. *MT2A* induction isn't necessarily bad; in fact, it can protect cells. The problem arises if *MT2A* gets switched on too strongly, or in a poorly controlled way, as this could interfere with the zinc-dependent signaling pathways, and disrupt immune

balance, potentially tipping what should be an adaptive response into something more pathological<sup>[9]</sup>. This line of thinking led to the proposal that *MT2A* might serve as a critical detective node at the intersection of zinc status and redox control, and that tracking *MT2A* could give us insights into COVID-19 severity while also helping us design better biomarker-driven treatment approaches.

To validate this hypothesis, two different approaches were brought together. First, a meta-analysis following PRISMA guidelines was conducted, looking at studies where COVID-19 patients received zinc supplements. Second, the gene expression data was analyzed, both bulk RNA-seq and single-cell RNA-seq from multiple body compartments: peripheral blood, lung tissue, bronchoalveolar lavage fluid, and sputum samples. The advantage of looking across all these compartments is that it helps us to determine which targets matter at different stages of disease, and aids the identification of host response that appear to be connected to zinc, and that can then be validated through more focused experiments.

## Materials and methods

### Meta analysis

The meta-analysis followed PRISMA guidelines, with full methodological details provided in the [Supplementary File 1](#)<sup>[10]</sup>. Studies involving hospitalized COVID-19 patients that compared outcomes between patients getting zinc supplements, and those

getting either a placebo or just standard care were referenced (Supplementary Table S1, Supplementary Fig. S1). The main focus was on mortality. Both randomized controlled trials and cohort studies were considered eligible. References included PubMed, Embase, Web of Science, the Cochrane Library, and ClinicalTrials.gov, with our final search conducted on September 3, 2024. Study selection, data extraction, and quality checks were all done independently by two reviewers; a third reviewer was used to make the final call over any disagreement. For assessing bias risk, the Cochrane tool was applied when evaluating RCTs, and ROBINS-I for studies that weren't randomized<sup>[11,12]</sup>. Depending on how much variation there was across the studies (heterogeneity), pooled odds ratios (ORs) were calculated with 95% confidence intervals (CIs), using either fixed-effects or random-effects models. Sensitivity analyses were also conducted and whether publication bias might be skewing the results was checked.

### Single-cell RNA sequencing data mining

The GSE158055 dataset was obtained from the GEO database ([www.ncbi.nlm.nih.gov/geo/](http://www.ncbi.nlm.nih.gov/geo/))<sup>[13]</sup>. 1,462,702 cells from 196 individuals were analyzed using a publicly available integrated h5 file. This included 22 mild/moderate cases, 54 severe, 95 convalescent COVID-19 patients, and 25 healthy controls. Samples were derived from peripheral blood mononuclear cell (PBMC) ( $n = 249$ ), bronchoalveolar fluid (BALF) ( $n = 12$ ), sputum ( $n = 22$ ), and pleural effusion ( $n = 1$ ). After standard quality control (removing cells with  $< 200$  genes,  $> 5\%$  mitochondrial reads, or  $> 2,500$  genes), 1,314,623 cells and 27,894 genes were retained, including 931,304 cells from PBMC, BALF, and sputum. These analyses were performed using Scanpy v1.9.6, NumPy v1.26.2, and pandas v1.5.1 in Python<sup>[14]</sup>.

### Bulk RNA-seq data mining

Two bulk RNA-seq datasets, GSE183533 and GSE198449, were downloaded from the GEO database ([www.ncbi.nlm.nih.gov/geo/](http://www.ncbi.nlm.nih.gov/geo/))<sup>[15,16]</sup>. For bulk RNA-seq analysis, expression matrices from GSE183533 (lung tissues from 31 COVID-19 decedents and nine controls) and GSE198449 (1,605 samples from 475 subjects across time points) were normalized to TPM. Transcriptome data from day 0, 1, 8, and 12, post-infection were analyzed. Differential expression was assessed using the limma package (v4.4.1). For visualization, gene expression data was standardized by z-scores and presented in heat maps using the R software.

### Protein-protein interaction analysis

PPI networks of MT2A were constructed using STRING software (<https://string-db.org/>). The minimum required interaction score was set to be greater than 0.4. The target protein was represented as a node in the network diagram.

### Gene set enrichment analysis (GSEA)

Patients with COVID-19 were divided into MT2A-high and MT2A-low groups using the median expression of MT2A as a cut-off. GSEA was performed using GSEAPy v1.0.2 in Python to find enriched Kyoto Encyclopedia of Genes and Genomes (KEGG) pathways<sup>[17]</sup>. Pathways with FDR  $< 0.05$  were obtained and the top 20 pathways with relatively higher NES were selected for display.

### Time-series analysis of gene expression clustering

Transcriptome sequencing from nine patients was completed with measurements at days 0, 1, 8, and 12 of SARS-CoV-2 infection,

and the average expression across these individuals obtained for trend-based clustering. These nine patients represent the subset of the original cohort with complete timepoints available for within-subject temporal analysis. Basic demographic and clinical descriptors for this subset (including age, sex, and clinical severity at sampling, were available in the GEO metadata) are summarized in Supplementary Table S2. Mfuzz v2.60.0 was used to automatically classify genes into seven clusters according to the trend of SARS-CoV-2 infection process by an unsupervised clustering method<sup>[18]</sup>. MT2A and genes involved in SARS-CoV-2 infection were also annotated.

### Statistical analysis

All statistical analyses were performed with the R package stats v4.4.1. The Wilcoxon rank sum test was used for comparison between the groups, and Spearman rank correlation analysis was used for correlation analysis. For analyses involving multiple comparisons,  $p$  values were adjusted using the Benjamini-Hochberg false discovery rate (FDR) procedure, and an FDR-adjusted  $p < 0.05$  was considered statistically significant.

## Results

### Clinical evidence: zinc supplementation is associated with reduced mortality

A total of 1,972 patients, ranging from infants to adults, were included in the analysis from seven studies<sup>[19–25]</sup>. Baseline characteristics of the study population are summarized in Supplementary Table S1. All seven studies met quality assessment standards (Supplementary Fig. S2a–S2d). Fixed-effects meta-analysis showed that zinc supplementation significantly reduced mortality risk (OR = 0.48; 95% CI: 0.36–0.64; Fig. 1a), with low heterogeneity and consistent findings across study designs (Supplementary Fig. S2e, S2f). Sensitivity analyses confirmed the robustness of this effect (pooled OR remained 0.48; Fig. 1b). No significant publication bias was detected (Egger's test,  $p = 0.43$ ; Supplementary Fig. S2).

### Target prioritization: MT2A is induced in monocytes in severe COVID-19

Initial analysis focused on the composition of immune cells in PBMCs with different severity and progression of COVID-19 at the single-cell transcriptome level (Fig. 2a–c). The proportions of monocytes, megakaryocytes, B cells, and plasma cells were increased, whereas the proportions of CD4<sup>+</sup> T cells and CD8<sup>+</sup> T cells were decreased during COVID-19 progression (Fig. 2d). The number of plasma cells increased significantly with disease progression, especially in severe cases. B cells and megakaryocytes were significantly increased in severe patients, whereas CD4<sup>+</sup> T cells, CD8<sup>+</sup> T cells, DCs, and NK cells were significantly decreased, especially in severe patients (Fig. 2e). The expression of zinc homeostasis-related genes showed that MT2A had the highest expression level in monocytes and macrophages. During disease progression, MT2A expression was lower in patients with moderate symptoms, but higher in patients with severe symptoms (Fig. 2f).

Subsequently, an analysis of the expression pattern of MT2A at the single-cell level was conducted (Fig. 3a–c). In monocytes, MT2A expression was decreased in the mild/moderate progression (MP) and mild/moderate convalescence (MC) groups, but increased in the severe/critical progression (SP) group (Fig. 3c). Correlation analysis

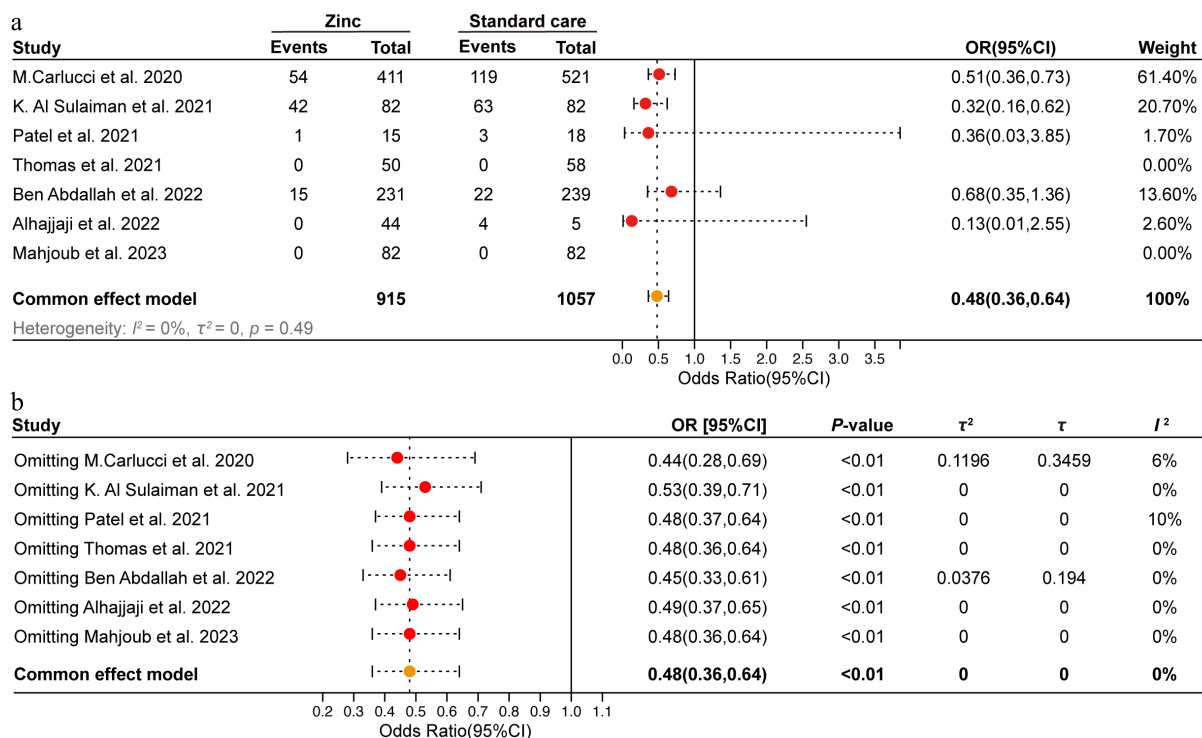


**Fig. 1** Meta-analysis of zinc supplementation on in-hospital mortality in COVID-19 patients. (a) Forest plot of in-hospital mortality of zinc supplementation and standard care groups. (b) Sensitivity analysis was conducted by sequentially excluding one study at a time to assess the robustness of the findings.

showed that *MT2A* expression in PBMCs was positively associated with most SARS-CoV-2 infection-related genes at the patient level among all groups (Fig. 3d). To further explore this association, the mean expression of each gene in monocytes per patient was calculated, and stratified patients into *MT2A*-high and *MT2A*-low groups, based on the median expression level (Fig. 3e-x). In both MP and SP groups, the *MT2A*-high subgroup showed significantly higher expression of *CTSB* and *IFIH1* compared to the *MT2A*-low group (Fig. 3f, l). In the MP group, *CTSL* and *TLR7* were also upregulated in the *MT2A*-high group (Fig. 3g, i). In contrast, in the SP group, *IL1B*, and *CCL3* were elevated in the *MT2A*-low group, whereas *TLR8* expression was higher in the *MT2A*-high group (Fig. 3j, n, w).

### Cross-compartment validation: *MT2A* associates with SARS-CoV-2 programs in BALF and sputum

Single-cell transcriptomic analysis on the BALF samples is shown (Fig. 4a-c). In BALF samples, the SP group showed increased proportions of monocytes, macrophages, and neutrophils compared to the MP group, while the proportions of NK cells, DCs, CD4+ T cells, CD8+ T cells, and B cells were decreased (Fig. 4d, e). *MT2A* expression in DCs was significantly higher in the SP group than in the MP group; conversely, *MT2A* in B cells, CD4+ T cells, CD8+ T cells, monocytes, macrophages, and epithelial cells was significantly lower in the SP group than in the MP group (Fig. 4f). *MT2A* was positively correlated with COVID-19-related genes, including *CTSB*, *CTSL*, *IFIH1*, *CCL2*, and *CXCL10*, in the SP group but not in the MP group (Fig. 4g). Mean expression of each gene in cells for each patient in the SP group was calculated. In epithelial cells, the mean expression of *CXCL10* showed higher expression in the *MT2A*-high group than in the *MT2A*-low group, although this difference did not remain significant after BH correction (Fig. 4h). In monocytes and macrophages, the

mean expression of *CTSL* and *CCL2* was significantly higher in the *MT2A*-high group than in the *MT2A*-low group (Fig. 4i, j). In macrophages, the mean expression of *CTSB* was significantly higher in the *MT2A*-high group compared to the *MT2A*-low group (Fig. 4i).

Subsequently, the characteristics of sputum samples were also analyzed (Fig. 4k-m). In sputum, the SP group has higher proportions of NK and epithelial cells but lower proportions of B cells than the MP group (Fig. 4n, o). Higher *MT2A* expression in epithelial cells and monocytes, and lower *MT2A* expression in DCs and macrophages were found in the SP group than in the MP group (Fig. 4p). *MT2A* expression was positively correlated with *IFIH1* and *GOLGA3* in the MP group and with *CTSB*, *IFIH1*, and *IL18* in the SP group (Fig. 4q). In monocytes, *TMPRSS2* showed a trend toward lower expression in the *MT2A*-high group compared with the *MT2A*-low group, although this difference did not remain significant after BH correction (Fig. 4r). Macrophages in the high *MT2A* group expressed less *IL1B* and *TNF* than those in the low *MT2A* group (Fig. 4s). Epithelial cells with higher *MT2A* levels expressed more *IL7* but less *IL10* than their counterparts with lower *MT2A* levels (Fig. 4t). DCs with higher *MT2A* levels expressed higher *CTSL* than their counterparts with lower *MT2A* levels (Fig. 4u).

### Lung tissue analysis: *MT2A* links to viral entry factors and inflammatory pathways in deceased patients

*MT2A* expression in lung tissue from deceased patients with COVID-19 was compared with healthy controls, based on bulk RNA-seq data. It was found that lung tissue from deceased patients with COVID-19 expressed higher levels of *MT2A*, and the remaining MTs showed a similar trend (Fig. 5a). Lung tissue from deceased COVID-19 patients with higher *MT2A* levels expressed lower *IFIH1* and *IL10* than those with lower *MT2A* levels (Fig. 5b, c). *MT2A* was positively

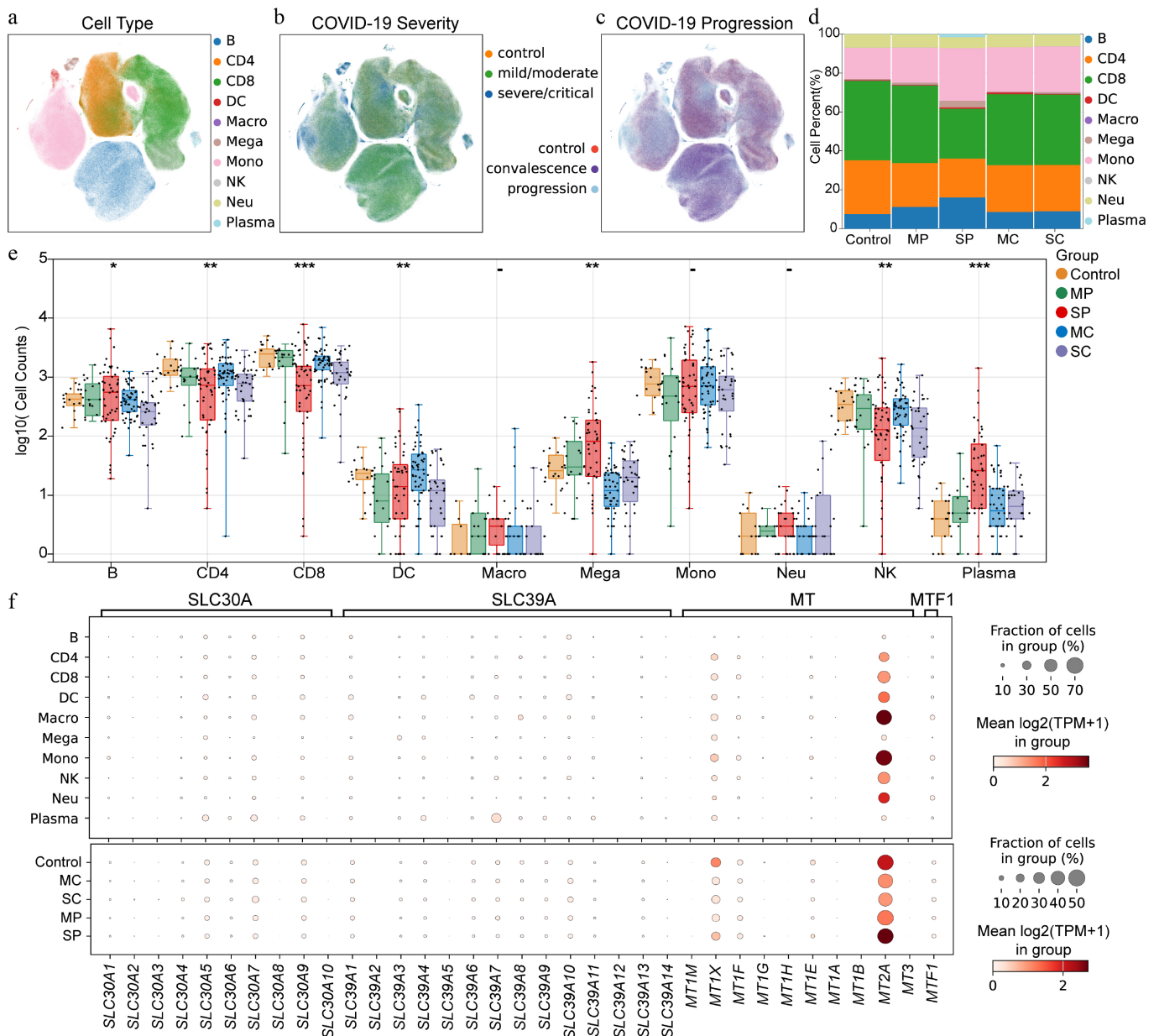


**Fig. 2** Expression pattern of zinc homeostasis related genes in PBMCs from patients with COVID-19 at single cell level. (a) Distribution of cell subpopulations. B indicates B cells, CD4 indicates CD4<sup>+</sup> T cells, CD8 indicates CD8<sup>+</sup> T cells, DC indicates dendritic cells, Macro indicates macrophages, Mega indicates megakaryocytes, Mono indicates monocytes, NK indicates natural killer cells, Neu indicates neutrophils, Plasma indicates plasma cells. (b) Cell distribution of COVID-19 samples with different severity. (c) Cell distribution of COVID-19 samples with disease progression. (d) Cell proportions in different status of COVID-19 patients. MP means mild/moderate progression. SP indicates severe/critical progression. MC indicates mild/moderate recovery. SC indicates severe/critical convalescence. (e) Number of immune cells in PBMC across different disease states of COVID-19 at the individual level. (f) Expression patterns of zinc homeostasis-related genes within different cell subpopulations and across different stages of COVID-19. Asterisks denote Benjamini–Hochberg FDR-adjusted *p* values (\* *p* < 0.05, \*\* *p* < 0.01, \*\*\* *p* < 0.001).

correlated with the SARS-CoV-2 infection-related genes *TMPRSS2* and *CTSL*, and negatively correlated with the inflammatory cytokines *IL10* and *IL18* in the lung tissue of deceased COVID-19 patients (Fig. 5d–g). Using the STRING database, we identified a PPI network centered on *MT2A*, involving other metallothioneins and proteins such as *STAT1* and *EOLA1* (Fig. 5h). GSEA indicated that *MT2A* may participate in neurodegenerative diseases, KEGG pathway: ko04610 (Complement and coagulation cascades), and multiple metabolic pathways (Fig. 5i, j), which should be interpreted as hypothesis-generating pending protein-level and functional validation.

### Temporal dynamics: *MT2A* peaks early in the blood during SARS-CoV-2 infection

Expression associations of *MT2A* and SARS-CoV-2 infection-related genes in peripheral blood samples showed that samples with higher *MT2A* expressed higher levels of *TMPRSS2*, *CTSBL*, *CTSL*, *TLR3*, *TLR7*, *IFIH1*, *GOLGA3*, *IL1B*, *TNF*, *CCL2*, *IL18*, *CXCL10*, *CSF1*, *CCL3*, and *IL10* than samples with lower *MT2A*. Conversely, peripheral blood samples with higher *MT2A* expressed lower *FURIN* than samples with low *MT2A* (Fig. 6a, b).

Changes in peripheral blood *MT2A* expression with the temporal phase of SARS-CoV-2 infection was examined. Importantly, *MT2A*

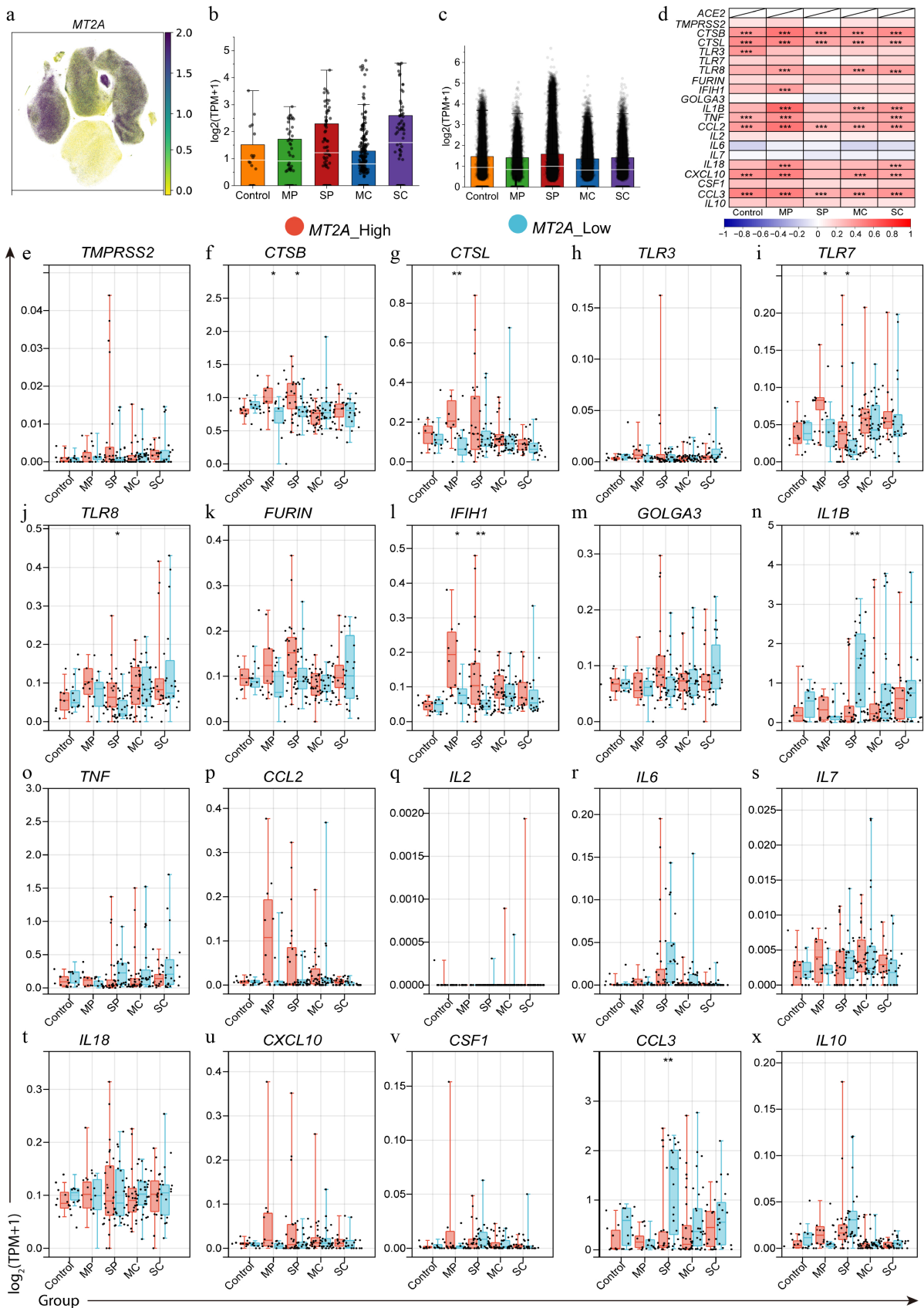


**Fig. 3** Differential expression of SARS-CoV-2 infection-related genes between *MT2A*-high and *MT2A*-low PBMC samples in different disease states. (a) *MT2A* expression in different cell types in PBMC samples from COVID-19 patients. *MT2A* expression levels in (b) macrophages, and (c) monocytes of different COVID-19 status. (d) Expression correlation between *MT2A* and SARS-CoV-2 infection-related genes in PBMCs of five groups. (e)-(x) The differential expression of various COVID-19-related genes between *MT2A*-high and *MT2A*-low monocytes under different disease status. Asterisks denote Benjamini-Hochberg FDR-adjusted  $p$  values (\*  $p < 0.05$ , \*\*  $p < 0.01$ , \*\*\*  $p < 0.001$ ).

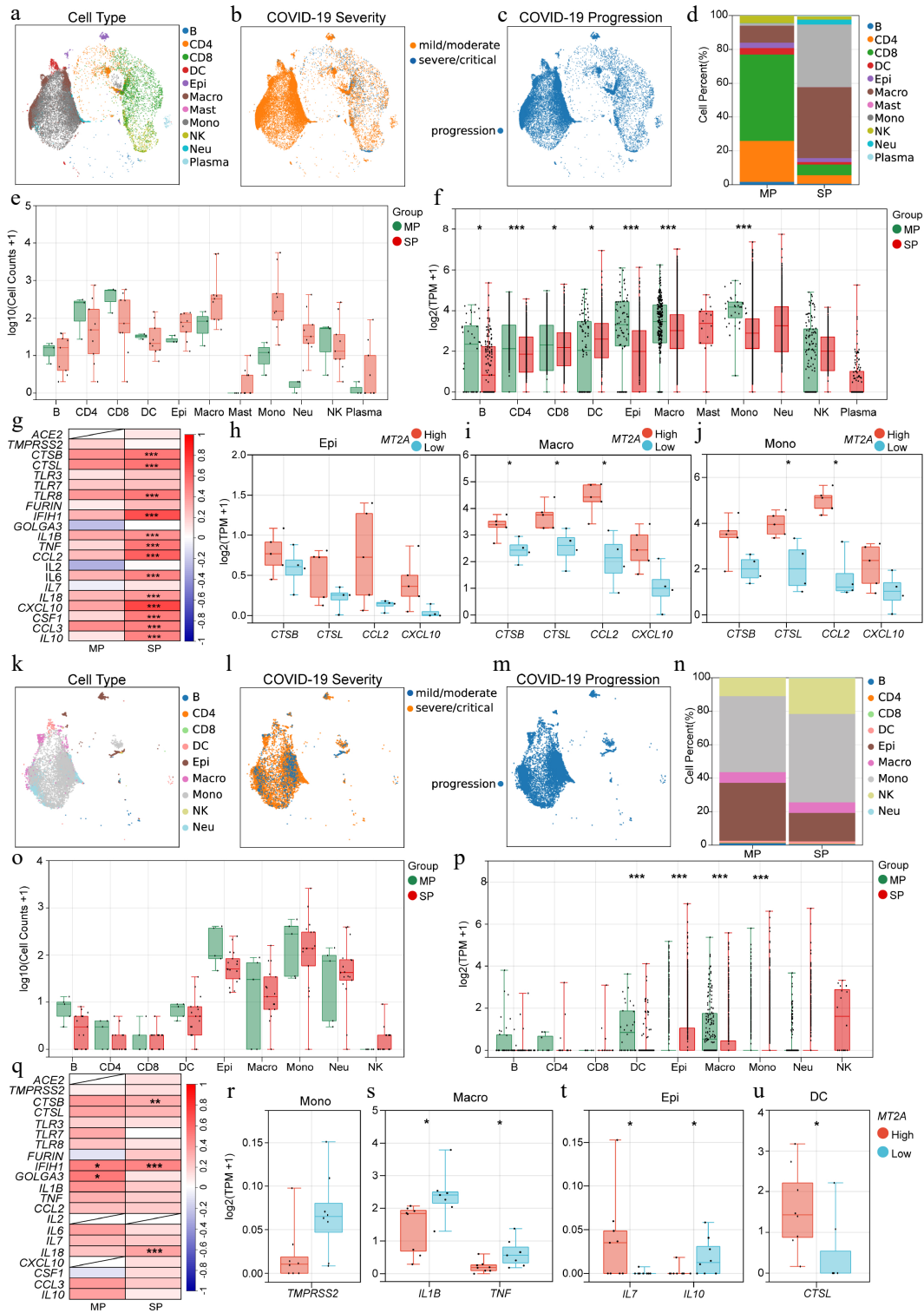


**Fig. 4** Association of *MT2A* and SARS-CoV-2 infection-related genes in BALF and sputum samples. Distribution of (a) immune cell types, (b) disease severity, and (c) progression status of BALF samples from COVID-19 patients. (d) Differential proportions, and (e) cell counts, of various immune cells in BALF between MP and SP groups. (f) *MT2A* expression in different immune cells between MP and SP groups. (g) Expression correlation between *MT2A* and SARS-CoV-2 infection-related genes in BALF of MP and SP groups. Differential expression genes between *MT2A*-high and *MT2A*-low (h) epithelial cells, (i) macrophages, and (j) monocytes in BALF. (k) Immune cell type distribution, (l) disease severity, and (m) progression status of sputum samples from COVID-19 patients. (n) Differential proportions, and (o) cell counts, of different immune cells in sputum samples between MP and SP groups. (p) *MT2A* expression in different immune cells between MP and SP groups. (q) Expression correlation between *MT2A* and SARS-CoV-2 infection-related genes in sputum samples of MP and SP groups. Differential expression genes between *MT2A*-high and *MT2A*-low (r) monocytes, (s) macrophages, (t) epithelial cells, and (u) DCs in sputum samples. Asterisks denote Benjamini-Hochberg FDR-adjusted *p* values (\* *p* < 0.05, \*\* *p* < 0.01, \*\*\* *p* < 0.001). For correlation analysis, \*\*\* means Benjamini-Hochberg FDR-adjusted *p* < 0.001, and absolute Spearman's correlation coefficient ≥ 0.3. Differential expression was assessed genome-wide within each cell type (*MT2A*-high vs *MT2A*-low).

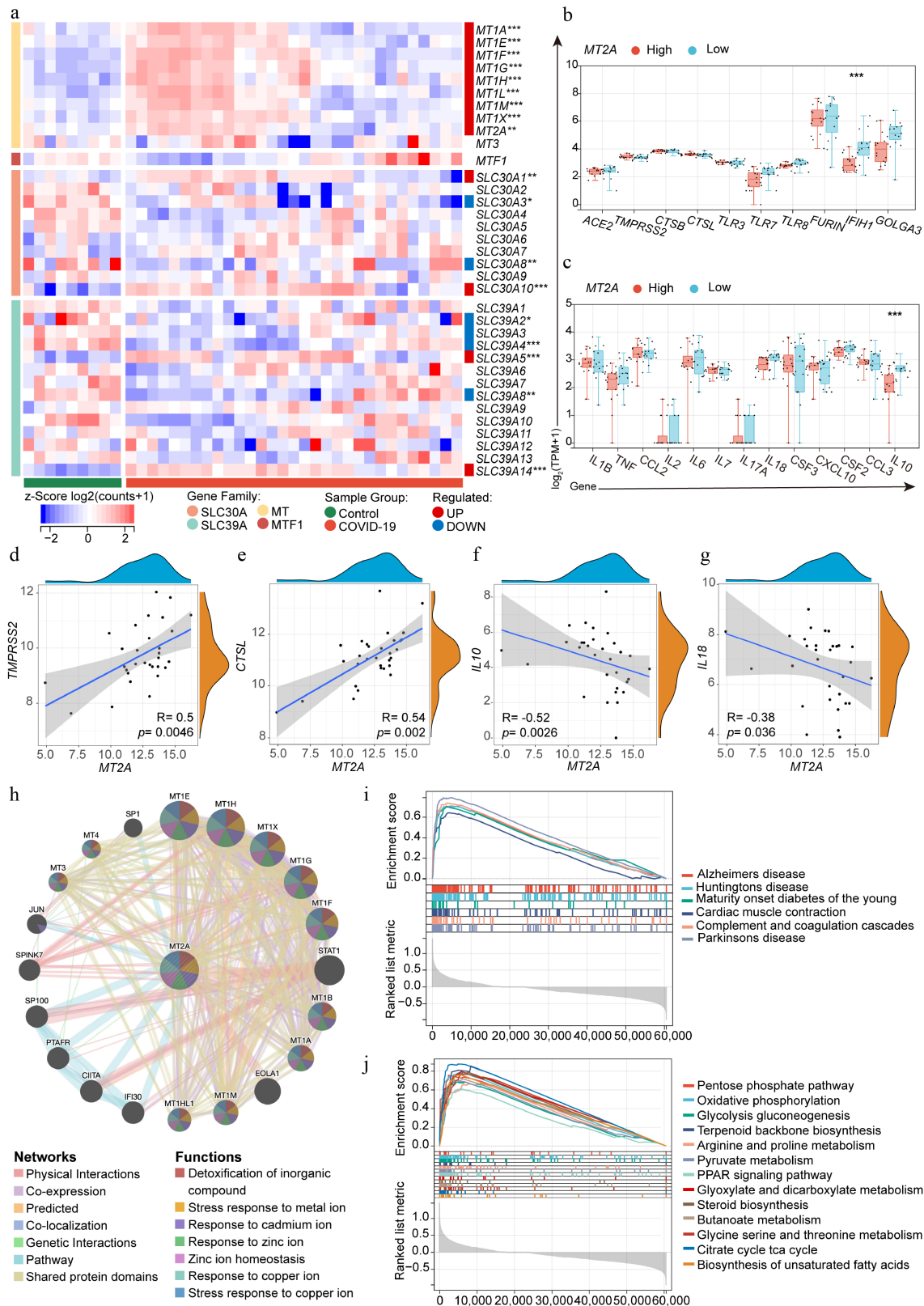


**Fig. 5** Lung *MT2A* expression and its association with SARS-CoV-2 infection-related genes. (a) Differential expression of zinc homeostasis-related genes in lung tissue from deceased COVID-19 patients ( $n = 31$ ) and normal controls ( $n = 9$ ). (b), (c) Differential expression of SARS-CoV-2 infection-related genes in *MT2A*-high and *MT2A*-low lung tissues from COVID-19 patients. Correlation of *MT2A* expression with (d) *TMPRSS2*, (e) *CTSL*, (f) *IL10*, and (g) *IL18* in the lungs of deceased COVID-19 patients. (h) The protein-protein interaction network centered on *MT2A* was identified using the STRING database. Lung tissues from COVID-19 patients were classified into *MT2A*-high and *MT2A*-low groups using the median expression of *MT2A* as a cut-off. Using the *MT2A*-low group as a control, (i) *MT2A*-associated diseases, and (j) cellular biological processes or pathways, were predicted using GSEA. These results were generated using the GSE183533 dataset from the GEO database. Asterisks denote Benjamini-Hochberg FDR-adjusted  $p$  values (\*  $p < 0.05$ , \*\*  $p < 0.01$ , \*\*\*  $p < 0.001$ ).

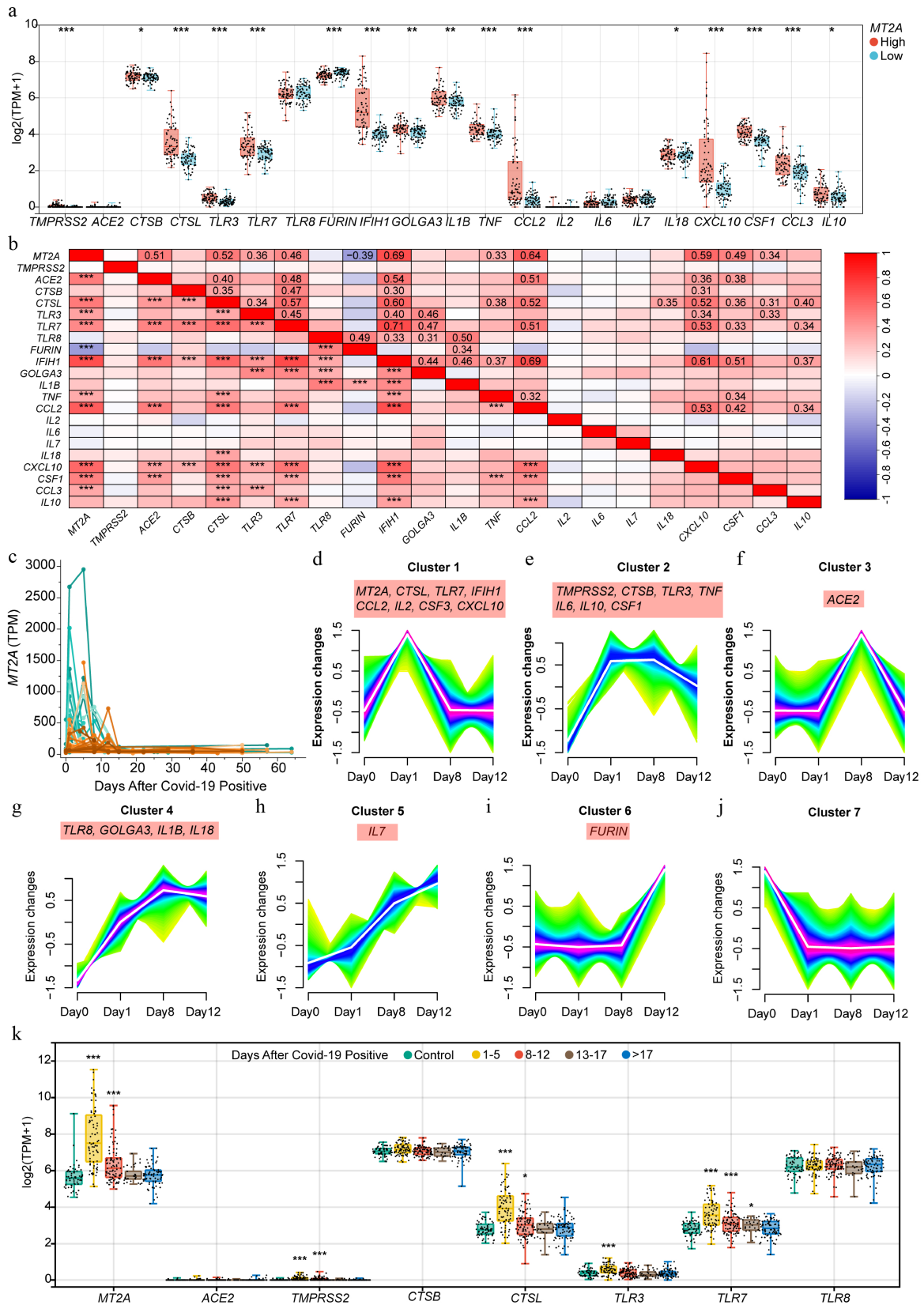


**Fig. 6** MT2A expression in peripheral blood and its association with SARS-CoV-2 infection-related genes during infection. (a) Differential expression of COVID-19-related genes between MT2A-high and MT2A-low peripheral blood samples from 338 specimens of 72 COVID-19 patients. (b) Correlation of expression levels of MT2A and SARS-CoV-2 infection-related genes. (c) Changes in peripheral blood MT2A expression levels during the course of infection in 72 COVID-19 patients. Seven gene clusters associated with (d) MT2A, and/or (e)–(j) COVID-19-related key genes based on expression similarity during SARS-CoV-2 infection in nine patients with complete timepoint data. (k) The expression changes of MT2A, ACE2, TMPRSS2, CTSB, CTSL, TLR3, TLR7, and TLR8 in different time periods after SARS-CoV-2 infection. Asterisks denote Benjamini–Hochberg FDR-adjusted  $p$  values (\*  $p < 0.05$ , \*\*  $p < 0.01$ , \*\*\*  $p < 0.001$ ). For correlation analysis, \*\*\* means Benjamini–Hochberg FDR-adjusted  $p < 0.001$ , and absolute Spearman's correlation coefficient  $\geq 0.3$ .

expression peaked at day 1 post-SARS-CoV-2 infection, and declined thereafter (Fig. 6c). Changes in *MT2A* during infection were highly consistent with a number of SARS-CoV-2 infection-associated genes, including *CTSL*, *TLR7*, *IFIH1*, *CCL2*, *IL2*, *CSF3*, and *CXCL10*. In contrast, the expression of *TMPRSS2*, *CTSB*, *TLR3*, *TNF*, *IL6*, *IL10*, and *CSF1* remained stable after an initial increase and then decreases (Fig. 6d–j). When the follow-up time is extended, the expression of *MT2A*, *TMPRSS2*, *CTSL*, *TLR3*, and *TLR7* show a significant increase during the early stage of infection and a decrease later in the infection process (Fig. 6k).

## Discussion

It's well established that zinc deficiency puts patients at higher risk of poor outcomes when they get viral infections. What remains less clear is which exactly which intracellular targets link systemic zinc levels to the immune programs that actually determine disease outcomes. Zinc influences antiviral immunity through several routes, it affects innate immune sensing, inflammatory signaling cascades, and the way cells handle stress<sup>[3,4]</sup>. This study combined evidence from clinical trials with detailed transcriptomic data from different tissue compartments, with the goal of pinpointing key zinc-related host factors in COVID-19. *MT2A* repeatedly appeared as a consistent signal tied to disease severity.

The meta-analysis results suggest that giving zinc supplements to hospitalized COVID-19 patients is associated with lower mortality (OR = 0.48, 95% CI: 0.36–0.64). Sensitivity checks were carried out, and the relationship held up, with low heterogeneity across studies. That said, drawing firm conclusions about zinc regimens need to be carefully considered, as the included studies were inconsistent in terms of what formulation they used, how much elemental zinc they gave, whether it was oral or intravenous, and how long treatment lasted. Instead of trying to say 'here's the perfect zinc protocol', the more important takeaway is mechanistic: we need to understand which intracellular nodes actually translate zinc availability into immune phenotypes that affect disease.

Metallothioneins are interesting because they do two things at once, they buffer zinc levels inside cells, and they link redox signals to zinc-dependent pathways. This puts the MT-zinc system at the crossroads of oxidative stress, metal handling, and immune function<sup>[26,27]</sup>. *MT2A* gets turned on in response to stress, and inflammatory cytokines like *IL6* and *TNF* can induce it, which fits with it behaving like an acute-phase protein during inflammation<sup>[28–30]</sup>. One thing worth noting is that *MT2A* doesn't respond exclusively to zinc. Other forms of metal stress or redox perturbations, for instance, when you chelate iron, which can also induce *MT2A*, and this overlaps with transcriptional programs linked to hypoxia and cellular stress<sup>[31]</sup>. Evidence tying MT biology to inflammatory signaling, especially pathways involving NF- $\kappa$ B, and this seems particularly relevant when oxidative stress is in play<sup>[29]</sup>. Taken together, it makes more sense to view *MT2A* as part of a feedback loop connecting inflammation, redox status, and zinc, rather than treating it as a simple readout that only responds to zinc.

*MT2A* doesn't just passively buffer zinc, if it gets induced too much, that could actually rewire zinc-dependent signaling in ways that contribute to harmful immune changes. Metallothioneins bind and release zinc dynamically in response to shifts in the redox environment, and when metallothionein levels change, that can alter the pool of loosely bound (labile) zinc inside cells. This labile pool controls a lot of transcriptional processes, including inflammatory pathways, where zinc availability makes a functional difference. Some earlier work has shown that metallothioneins can modulate

NF- $\kappa$ B activity in a zinc-dependent fashion, which supports the notion that if *MT2A* gets overexpressed, it might change how sensitive cells are to inflammatory signals, and how long those inflammatory transcription programs stay active<sup>[32,33]</sup>. When a protein interaction network centered on *MT2A* in lung tissue using STRING was investigated, it was found to include *STAT1* and *EOLA1*, which fits with the broader systems-level coupling proposed here. This suggests possible connections between interferon signaling and to inflammatory regulation in endothelial cells, *EOLA1* in particular has been reported to modulate *IL-6*-related inflammatory responses in endothelial contexts<sup>[34]</sup>. When GSEA was run on lung tissue with high *MT2A* expression, complement, and coagulation pathways appeared, which makes sense given the thromboinflammatory phenotype you see in severe COVID-19, and the known coupling between inflammatory gene activation and prothrombotic vascular programs<sup>[35]</sup>. Interestingly, GSEA also flagged neurodegeneration-related gene sets. This might reflect overlap between systemic inflammation, redox/metal stress, and neurovascular or neuroinflammatory processes during acute infection. There is growing evidence that SARS-CoV-2 can disrupt gliovascular integrity and trigger neuroinflammatory responses, and zinc–metallothionein stress pathways have been implicated in neurodegenerative disease mechanisms. These observations raise the hypothesis that excessive or prolonged *MT2A* induction could overlap with pathways relevant to post-acute neurological problems in vulnerable patients<sup>[36,37]</sup>. It is important to emphasize that these are hypothesis-generating observations which need to be validated through perturbation experiments where zinc is carefully controlled.

In peripheral blood, *MT2A*-high samples expressed higher levels of infection-related genes spanning entry/processing factors (*TMPRSS2*, *CTSB*, *CTSL*; with lower *FURIN*), innate sensing (*TLR3*, *TLR7*, *IFIH1*), and inflammatory mediators (*IL1B*, *TNF*, *CCL2*, *IL18*, *CXCL10*, *CSF1*, *CCL3*, *IL10*). This is notable because SARS-CoV-2 entry can proceed via *TMPRSS2*-mediated plasma membrane activation and cathepsin B/L-dependent endosomal activation, and experimental and modeling work supports the relevance of these parallel routes and the potential benefit of dual-route targeting<sup>[38,39]</sup>. *CTSL* has been reported as clinically relevant in COVID-19 and mechanistically important for infection, reinforcing the plausibility that *MT2A*-linked programs intersect with entry-associated protease pathways<sup>[40]</sup>. Importantly, transcriptome co-variation does not establish direct regulation; a parsimonious interpretation is that *MT2A* marks a broader inflammatory/redox stress state in which entry-related and inflammatory programs are altered in coordination. Within such a state, *MT2A*-mediated zinc buffering could modulate signaling thresholds and inflammatory amplification without implying direct control of each downstream gene<sup>[3,26]</sup>.

Longitudinal analyses further refine the temporal context of *MT2A* regulation. *MT2A* expression peaked at day 1 post-infection and declined thereafter, and its trajectory broadly co-varied with infection-associated programs including *CTSL*, *TLR7*, *IFIH1*, *CCL2*, *IL2*, *CSF3*, and *CXCL10*. With extended follow-up, *MT2A* and several infection-linked genes showed an early increase, followed by a later decrease, consistent with *MT2A* behaving as an inducible responder during the early inflammatory phase. Co-variation with *TLR7/IFIH1*-linked sensing is biologically plausible given the central role of early interferon pathways and endosomal RNA sensing in COVID-19 trajectories, and evidence linking impaired *TLR7* signaling to severe disease<sup>[41,42]</sup>. At the same time, the Mfuzz-based trajectory clustering relies on a small subset ( $n = 9$ ), and should be treated as preliminary. Larger longitudinal cohorts, with denser sampling and harmonized clinical annotation, will be needed to quantify inter-individual variability, and to test whether *MT2A* dynamics associate with

severity progression, protein-level inflammation, or response to zinc-related interventions.

A key theme from the present cross-compartment analyses is that *MT2A* regulation is compartment- and cell-type-specific. Elevated *MT2A* was observed in systemic monocytes, whereas *MT2A*-associated patterns differed across local respiratory niches such as bronchoalveolar lavage fluid and sputum. Several non-mutually exclusive mechanisms could contribute: differences in zinc bioavailability and transporter activity, local cytokine/interferon tone, oxidative stress and hypoxia/tissue-injury cues, and lineage differentiation states shaped by the airway microenvironment<sup>[3,43]</sup>. These considerations argue for a compartment-aware evaluation of *MT2A* biology, and for caution when extrapolating signals from blood to airway niches.

Severe COVID-19 involves both immune-cell compositional remodeling and lineage-specific transcriptional reprogramming. Although plasma cells and megakaryocytes expand and T-cell fractions contract, *MT2A* dysregulation is most prominent in myeloid compartments, supporting a lineage-restricted zinc/redox stress program rather than a universal immune-wide driver. Abundance shifts and gene-expression programs can be partially decoupled: expanded lineages with modest *MT2A* may contribute via *MT2A*-independent mechanisms, whereas myeloid populations can exert disproportionate effects through inflammatory amplification. Accordingly, *MT2A* is best positioned as a myeloid-linked enrichment/monitoring biomarker and a candidate host node with context- and cell-type-dependent translational relevance. Across bronchoalveolar lavage fluid and sputum, co-variation with cathespins (e.g., *CTSB/CTSL*) is best viewed as a stress-linked endosomal/lysosomal program, not as evidence that zinc supplementation promotes viral invasion. This interpretation needs direct testing under standardized zinc manipulation, including depletion/chelation and rescue designs, rather than inference from observational co-expression<sup>[44]</sup>.

Mechanism remains an open question. Because *MT2A* is inducible by cytokines and oxidative stress, elevated *MT2A* in severe COVID-19 could be downstream of inflammation rather than an upstream driver<sup>[28,29]</sup>. A coherent synthesis is a context-dependent feedback model: inflammatory stress induces *MT2A* as part of an acute adaptive response, while *MT2A*-mediated zinc buffering and redox coupling may secondarily modulate signaling thresholds that shape entry-related and inflammatory outputs under specific zinc states<sup>[3,26]</sup>. Disentangling 'responder vs regulator' roles will require perturbation-based validation with controlled zinc manipulation and time-resolved readouts.

Two translational directions follow from these data. First, peripheral *MT2A* expression in monocytes may serve as an enrichment and monitoring biomarker of a zinc-linked redox-immune stress state, potentially reducing clinical heterogeneity in zinc intervention trials. Second, *MT2A* represents a candidate host node for targeted modulation of its expression or zinc-binding dynamics. Direct interventional evidence supporting *MT2A*-targeted therapy in acute viral illness is currently lacking, so the therapeutic concept remains hypothesis-generating. Establishing plausibility will require perturbation studies in myeloid systems that couple *MT2A* knock-down/overexpression with spike-mediated or pseudovirus entry assays, quantify *TMPRSS2/CTSL/CTSB* at both mRNA and protein levels, and measure inflammatory outputs under standardized zinc supplementation and zinc depletion/chelation with rescue designs. Where feasible, *Mt2*-deficient infection models (global or myeloid-specific) can then assess *in vivo* relevance using viral burden, lung pathology, cytokine profiles, and downstream coagulation and complement readouts.

Despite a strong disease association, *MT2A* is not an 'easy' target. As an intracellular zinc-buffering protein without a canonical enzymatic active site, it is less amenable to conventional small-molecule inhibition, and redundancy across metallothionein isoforms complicates specificity. Any acute-infection intervention would likely need to be time-limited and cell-type aware to mitigate safety liabilities. Nevertheless, feasibility precedents exist. Metallothionein suppression has been explored *via* gene-silencing approaches, including reports that metallothionein knockdown modulates cisplatin resistance in malignant pleural mesothelioma and that *MT2A* knockdown alters invasive phenotypes in cancer models<sup>[45]</sup>. Targeted delivery concepts such as phi29 pRNA-based platforms carrying siRNA against *MT2A* have been reported<sup>[46]</sup>. More recently, a first-in-class *MT2A* degrader has been described, suggesting direct protein-level modulation may be technically achievable, although relevance and safety in acute viral illness remain untested<sup>[47]</sup>. Collectively, these considerations support prioritizing *MT2A* first as an enrichment/monitoring biomarker while *MT2A*-modulating modalities are pursued as longer-term host-directed strategies contingent on perturbation-based efficacy and safety validation.

This study has several limitations. First, integrated public transcriptomic analyses are inherently associative; causal validation in *MT2A*-perturbation or knockout systems is required to establish the mechanism. Second, the meta-analysis includes heterogeneous zinc regimens in formulation, elemental dose, route, and duration, complicating regimen-level translation and underscoring the need for standardized protocols and biomarker-guided dosing in future trials. Third, *MT2A* regulation is compartment- and cell-type-specific, and the molecular drivers of tissue heterogeneity remain incompletely defined. Fourth, sample size and follow-up constraints limit generalizability to sparsely represented subgroups and preclude direct evaluation of *MT2A* in post-acute sequelae. Fifth, single-cell and bulk RNA-seq capture gene-expression associations and pathway enrichment rather than protein abundance, localization, or functional activity; targeted protein-level and functional validation will be important, particularly for entry-related factors and inflammatory mediators.

## Conclusions

In summary, a PRISMA-guided meta-analysis was combined with transcriptomic profiling across multiple tissue compartments to map out a zinc-related host network in COVID-19. Through that work, *MT2A* was identified as a reproducible node associated with disease severity. The meta-analysis showed that zinc supplementation was linked to lower in-hospital mortality, while elevated *MT2A*, especially in myeloid cells, tracked with a co-regulated program connected to SARS-CoV-2 entry/processing and inflammatory signaling. The longitudinal blood data further indicated that *MT2A* is induced transiently early in infection, which highlights how its role is stage-dependent. Overall, these findings support the idea that *MT2A* could serve as a biomarker of metal/redox-immune stress and as a host target we can validate experimentally. They provide a rationale for moving forward with perturbation-based validation studies under controlled zinc conditions, and for setting up prospective biomarker-stratified trials, to determine whether *MT2A* is useful for enriching patient populations and deciding when to intervene.

## Ethical statements

The data used in this study were provided by the Gene Expression Omnibus (GEO) database (Accession Nos GSE158055, GSE183533, and GSE198449), and public literature databases

(PubMed, Embase, Web of Science, Cochrane Library, and Clinical-Trials.gov). Therefore, no ethics committee approval or informed consent was required for this study.

## Author contributions

The authors confirm contributions to the paper as follows: study conception and design: Zhu B, Hua S, Li Z; data collection: Li Z, Hua S, Zhu B, Luo Y; analysis and interpretation of results: Li Z, Hua S, Zhu B, Luo Y, Qian W, Song S, Li J; draft manuscript preparation: Zhu B, Li Z, Hua S, Liu L. All authors reviewed the results and approved the final version of the manuscript.

## Data availability

Raw bulk or single-cell RNA-seq data supporting this study are publicly available from the GEO database ([www.ncbi.nlm.nih.gov/geo](http://www.ncbi.nlm.nih.gov/geo)) under accession numbers GSE158055, GSE183533, and GSE198449. All other datasets generated and/or analyzed during the current study are available from the corresponding author upon reasonable request

## Acknowledgments

Not applicable.

## Conflict of interest

The authors declare no competing interests.

**Supplementary information** accompanies this paper online at: <https://doi.org/10.48130/targetome-0026-0006>.

## Dates

Received 18 December 2025; Revised 18 January 2026; Accepted 26 January 2026; Published online 13 February 2026

## References

- [1] Aw DZH, Zhang DX, Vignuzzi M. 2025. Strategies and efforts in circumventing the emergence of antiviral resistance against conventional antivirals. *npj Antimicrobials and Resistance* 3:54
- [2] Nature Microbiology. 2024. Considering the host in host-pathogen interactions. *Nature Microbiology* 9:1149–49
- [3] Chen B, Yu P, Chan WN, Xie F, Zhang Y, et al. 2024. Cellular zinc metabolism and zinc signaling: from biological functions to diseases and therapeutic targets. *Signal Transduction and Targeted Therapy* 9:6
- [4] Read SA, Obeid S, Ahlenstiel C, Ahlenstiel G. 2019. The role of zinc in antiviral immunity. *Advances in Nutrition* 10:696–710
- [5] Jothimani D, Kailasam E, Danielraj S, Nallathambi B, Ramachandran H, et al. 2020. COVID-19: poor outcomes in patients with zinc deficiency. *International Journal of Infectious Diseases* 100:343–49
- [6] Santos HO. 2022. Therapeutic supplementation with zinc in the management of COVID-19-related diarrhea and ageusia/dysgeusia: mechanisms and clues for a personalized dosage regimen. *Nutrition Reviews* 80:1086–1093
- [7] Briassoulis G, Briassoulis P, Iliia S, Miliaraki M, Briassoulis E. 2023. The anti-oxidative, anti-inflammatory, anti-apoptotic, and anti-necroptotic role of zinc in COVID-19 and sepsis. *Antioxidants* 12:1942
- [8] Chu A, Foster M, Ward S, Zaman K, Hancock D, et al. 2015. Zinc-induced upregulation of metallothionein (MT)-2A is predicted by gene expression of zinc transporters in healthy adults. *Genes & Nutrition* 10:44
- [9] Kwon CS, Kountouri AM, Mayer C, Gordon MJ, Kwun IS, et al. 2007. Mononuclear cell metallothionein mRNA levels in human subjects with poor zinc nutrition. *The British Journal of Nutrition* 97:247–254
- [10] Page MJ, McKenzie JE, Bossuyt PM, Boutron I, Hoffmann TC, et al. 2021. The PRISMA 2020 statement: an updated guideline for reporting systematic reviews. *BMJ* 372:n71
- [11] Sterne JA, Hernán MA, Reeves BC, Savović J, Berkman ND, et al. 2016. ROBINS-I: a tool for assessing risk of bias in non-randomised studies of interventions. *BMJ* 355:i4919
- [12] Higgins JPT, Altman DG, Gøtzsche PC, Jüni P, Moher D, et al. 2011. The Cochrane Collaboration's tool for assessing risk of bias in randomised trials. *BMJ* 343:d5928
- [13] Ren X, Wen W, Fan X, Hou W, Su B, et al. 2021. COVID-19 immune features revealed by a large-scale single-cell transcriptome atlas. *Cell* 184:1895–913.e19
- [14] Wolf FA, Angerer P, Theis FJ. 2018. SCANPY: large-scale single-cell gene expression data analysis. *Genome Biology* 19:15
- [15] Sauerwald N, Zhang Z, Ramos I, Nair VD, Soares-Schanoski A, et al. 2022. Pre-infection antiviral innate immunity contributes to sex differences in SARS-CoV-2 infection. *Cell Systems* 13:924–31.e4
- [16] Budhreja A, Basu A, Gheware A, Abhilash D, Rajagopala S, et al. 2022. Molecular signature of postmortem lung tissue from COVID-19 patients suggests distinct trajectories driving mortality. *Disease Models & Mechanisms* 15:dmm049572
- [17] Fang Z, Liu X, Peltz G. 2023. GSEAPy: a comprehensive package for performing gene set enrichment analysis in Python. *Bioinformatics* 39:btac757
- [18] Futschik ME, Carlisle B. 2005. Noise-robust soft clustering of gene expression time-course data. *Journal of Bioinformatics and Computational Biology* 3:965–88
- [19] Mahjoub L, Youssef R, Yaakoubi H, Ben Salah H, Jaballah R, et al. 2024. Melatonin, vitamins and minerals supplements for the treatment of Covid-19 and Covid-like illness: a prospective, randomized, double-blind multicenter study. *Explore* 20:95–100
- [20] Thomas S, Patel D, Bittel B, Wolski K, Wang Q, et al. 2021. Effect of high-dose zinc and ascorbic acid supplementation vs usual care on symptom length and reduction among ambulatory patients with SARS-CoV-2 infection: the COVID A to Z randomized clinical trial. *JAMA Network Open* 4:e210369–e69
- [21] Ben Abdallah S, Mhalla Y, Trabelsi I, Sekma A, Youssef R, et al. 2023. Twice-daily oral zinc in the treatment of patients with coronavirus disease 2019: a randomized double-blind controlled trial. *Clinical Infectious Diseases* 76:185–191
- [22] Patel O, Chinni V, El-Khoury J, Perera M, Neto AS, et al. 2021. A pilot double-blind safety and feasibility randomized controlled trial of high-dose intravenous zinc in hospitalized COVID-19 patients. *Journal of Medical Virology* 93:3261–3267
- [23] Ibrahim Alhajjaji G, Alotaibi N, Abutaleb N, Alotaibi MM, Alhajjaji A, et al. 2023. Effect of zinc supplementation on symptom reduction and length of hospital stay among pediatric patients with Coronavirus disease 2019 (COVID-19). *Saudi Pharmaceutical Journal* 31:585–591
- [24] Al Sulaiman K, Aljuhani O, Al Shaya AI, Kharbosh A, Kensara R, et al. 2021. Evaluation of zinc sulfate as an adjunctive therapy in COVID-19 critically ill patients: a two center propensity-score matched study. *Critical Care* 25:363
- [25] Carlucci PM, Ahuja T, Petrilli C, Rajagopalan H, Jones S, et al. 2020. Zinc sulfate in combination with a zinc ionophore may improve outcomes in hospitalized COVID-19 patients. *Journal of Medical Microbiology* 69:1228–1234
- [26] Maret W, Krezel A. 2007. Cellular zinc and redox buffering capacity of metallothionein/thionein in health and disease. *Molecular Medicine* 13:371–375
- [27] Subramanian Vignesh K, Deepe GS, Jr. 2017. Metallothioneins: emerging modulators in immunity and infection. *International Journal of Molecular Sciences* 18:2197
- [28] Sato M, Sasaki M, Hojo H. 1994. Differential induction of metallothionein synthesis by interleukin-6 and tumor necrosis factor- $\alpha$  in rat tissues. *International Journal of Immunopharmacology* 16:187–195
- [29] Ling XB, Wei HW, Wang J, Kong YQ, Wu YY, et al. 2016. Mammalian metallothionein-2A and oxidative stress. *International Journal of Molecular Sciences* 17:1483

- [30] Butcher HL, Kennette WA, Collins O, Zalups RK, Koropatnick J. 2004. Metallothionein mediates the level and activity of nuclear factor kappa B in murine fibroblasts. *The Journal of Pharmacology and Experimental Therapeutics* 310:589–598
- [31] Saletta F, Suryo Rahmanto Y, Noulisri E, Richardson DR. 2010. Iron Chelator-mediated alterations in gene expression: identification of novel iron-regulated molecules that are molecular targets of hypoxia-inducible factor-1 $\alpha$  and p53. *Molecular Pharmacology* 77:443–458
- [32] Kim CH, Kim JH, Lee J, Ahn YS. 2003. Zinc-induced NF- $\kappa$ B inhibition can be modulated by changes in the intracellular metallothionein level. *Toxicology and Applied Pharmacology* 190(2):189–196
- [33] Stafford SL, Bokil NJ, Achard MES, Kapetanovic R, Schembri MA, et al. 2013. Metal ions in macrophage antimicrobial pathways: emerging roles for zinc and copper. *Bioscience Reports* 33:e00049
- [34] Liu Y, Liu H, Chen W, Yang T, Zhang W. 2014. EOLA1 protects lipopolysaccharide induced IL-6 production and apoptosis by regulation of MT2A in human umbilical vein endothelial cells. *Molecular and Cellular Biochemistry* 395:45–51
- [35] Mussbacher M, Salzman M, Brostjan C, Hoesel B, Schoergenhofer C, et al. 2019. Cell type-specific roles of NF- $\kappa$ B linking inflammation and thrombosis. *Frontiers in Immunology* 10:85
- [36] Fekete R, Simats A, Bíró E, Pósfai B, Cserép C, et al. 2025. Microglia dysfunction, neurovascular inflammation and focal neuropathologies are linked to IL-1- and IL-6-related systemic inflammation in COVID-19. *Nature Neuroscience* 28:558–576
- [37] Beckers M, Bloem BR, Helmich RC. 2023. Mask on, mask off: subclinical Parkinson's disease unveiled by COVID-19. *Journal of Movement Disorders* 16:55–58
- [38] Padmanabhan P, Desikan R, Dixit NM. 2020. Targeting TMPRSS2 and Cathepsin B/L together may be synergistic against SARS-CoV-2 infection. *PLoS Computational Biology* 16:e1008461
- [39] Hashimoto R, Sakamoto A, Deguchi S, Yi R, Sano E, et al. 2021. Dual inhibition of TMPRSS2 and Cathepsin B prevents SARS-CoV-2 infection in iPSC cells. *Molecular Therapy Nucleic Acids* 26:1107–1114
- [40] Zhao MM, Yang WL, Yang FY, Zhang L, Huang WJ, et al. 2021. Cathepsin L plays a key role in SARS-CoV-2 infection in humans and humanized mice and is a promising target for new drug development. *Signal Transduction and Targeted Therapy* 6:134
- [41] van der Made CI, Simons A, Schuurs-Hoeijmakers J, van den Heuvel G, Mantere T, et al. 2020. Presence of genetic variants among young men with severe COVID-19. *JAMA* 324:663–673
- [42] Wang C, Khatun MS, Ellsworth CR, Chen Z, Islamuddin M, et al. 2024. Deficiency of Tlr7 and Irf7 in mice increases the severity of COVID-19 through the reduced interferon production. *Communications Biology* 7:1162
- [43] Lynes MA, Hidalgo J, Manso Y, Devisscher L, Laukens D, et al. 2014. Metallothionein and stress combine to affect multiple organ systems. *Cell Stress and Chaperones* 19:605–611
- [44] Duprez J, Roma LP, Close AF, Jonas JC. 2012. Protective antioxidant and antiapoptotic effects of ZnCl<sub>2</sub> in rat pancreatic islets cultured in low and high glucose concentrations. *PLoS One* 7:e46831
- [45] Borchert S, Suckrau PM, Walter RFH, Wessolly M, Mairinger E, et al. 2020. Impact of metallothionein-knockdown on cisplatin resistance in malignant pleural mesothelioma. *Scientific Reports* 10:18677
- [46] Tarapore P, Shu Y, Guo P, Ho SM. 2011. Application of phi29 motor pRNA for targeted therapeutic delivery of siRNA silencing metallothionein-IIA and survivin in ovarian cancers. *Molecular Therapy* 19:386–394
- [47] Racioppo B, Pechalrieu D, Abegg D, Dwyer B, Ramseier NT, et al. 2025. Chemoproteomics-enabled de novo proteolysis targeting chimera discovery platform identifies a metallothionein degrader to probe its role in cancer. *Journal of the American Chemical Society* 147:7817–7828



Copyright: © 2026 by the author(s). Published by Maximum Academic Press on behalf of China Pharmaceutical University. This article is an open access article distributed under Creative Commons Attribution License (CC BY 4.0), visit <https://creativecommons.org/licenses/by/4.0/>.